PHYSICAL REVIEW A VOLUME 15, NUMBER 2 FEBRUARY 1977

X-ray spectra from exploded-wire plasmas*

P. G. Burkhalter, C. M. Dozier, and D. J. Nagel
Naval Research Laboratory, Washington, D. C. 20375
(Received 8 July 1976)

X-ray line spectra were collected from exploded (Al to U) wire plasmas produced by 10^{12}-W pulse discharges of high-energy electrons in the Gamble II generator. High-ionization states were found in these spectra that provided new spectroscopic data. The Ne- and Ni-like isoelectronic sequences involving L- and M-shell transitions were extended to high-atomic-number elements, Ag and Au, respectively. The correlation of spectra and x-ray pinhole images revealed that the high-temperature emission emanates from small (< 75 μm), high-density pinched regions with plasma temperatures of 1–2 keV (based on the coronal model). Other x-ray emission arises from cool-plasma (50–200 eV) regions associated with the flaring structure as seen in x-ray-pinhole images. In addition to low-temperature thermal x-ray emission from the flare regions, energetic electrons produce nonthermal inner-shell spectral lines. As the atomic number increases, the relative intensity of the cool plasma to high-temperature thermal emission increases systematically for isoelectronic sequences involving K-, L-, and M-shell transitions. The plasma characteristics determined from the distribution of ionization states in the exploded-wire spectra correlate well with those from other high-energy-density generating devices, namely the vacuum spark and plasma focus.

I. INTRODUCTION

The emission of electromagnetic radiation which results from electrically heating thin wires very suddenly is a well-known phenomenon. Between 1958 and 1967 four conferences were held which dealt exclusively with the exploding-wire phenomenon.[1] Low-voltage, electron discharge currents cause wires to dissociate or melt, yielding infrared or visible radiation.[2,3] High-energy electron beams produce exploding wires which radiate in the extreme ultraviolet and the x-ray region from <1 to 15 keV.[4-6] In recent years, intense x-ray line emission has resulted from discharging the 10^{12}-W, relativistic-electron Gamble II generator.[7-10] The x-ray line emission is composed of both thermal and nonthermal x-ray spectra which have been ascribed to the pinches and flare structure observed in x-ray pinhole images of the exploded wires. The x-ray spectra from exploded wires (EW) are found to have some of the highest ionization states that have so far been observed in high-Z elements.[11-13]

In this study, x-ray spectra and pinhole images have been collected throughout the Periodic Table. The spectra were recorded in the 1–12-keV region with curved-crystal x-ray spectrographs. The x-ray line spectra have been studied in detail to identify the various ionization states. The plasma conditions necessary to generate these spectra have been determined, in part, from the degree of ionization achieved for each wire exploded. The length and width of the spectral lines, relative line intensities, and correlation of the x-ray spectra with x-ray pinhole images have increased our understanding of the origin of the various x-ray emissions in exploded wires. In addition, new spectrographic data for highly ionized, high-Z elements were acquired.

II. EXPERIMENTAL

The production of electrical pulses in the Gamble II generator has been previously described by Mosher *et al.*[9] Basically a 220-kJ Marx-capacitor bank is used to charge a single, large, water capacitor. This capacitor discharges into a water dielectric coaxial transmission line that tapers to a 1.5-Ω output resistance at the point where the pulse is extracted into the diode. Thin wires or ribbons are stretched between the electrode gap in the vacuum diode. About 50 kJ of high-energy electrons discharge into the plasma created from the wire in pulse durations of about 80 nsec. The preplasma results from the early part of the electrical discharge which causes the wire to rapidly vaporize uniformly along its entire length, as shown by streak-camera photographs. The initially 1-MeV energetic electrons rapidly dissipate their energy in plasma interactions. However, there is evidence that energetic electrons are available in the exploded wires throughout the pulse duration. A portion of the wires is viewed simultaneously by an x-ray pinhole camera and two crystal spectrographs mounted on opposite parts of the inter-electrode vacuum chamber. The geometry is schematically illustrated in Fig. 1.

Thin wires of elements throughout the Periodic Table from CH_2 to U were exploded to record spectral information. X-ray data were collected from pure-element wires of Al, Ti, Fe, Cu, Mo,

Ag, W, Au, and U and also compounds like Saran $(C_2H_3Cl)_n$ and alloys like Pt–13%-Rh thermocouple wire. The wires range from 12 to 127 μm in diameter while the ribbons had a rectangular cross section typically 25×75 μm. All of the spectral data used in this report were from wires 25 to 50 μm in diameter.

X-ray pinhole images were recorded on most of the shots for aiding in the interpretation of the spectral data and also to determine whether a good shot occurred. This was generally indicated by a regular array of pinches along the original wire position together with the production of thermal x-ray spectral patterns. Pinhole photographs were collected at a magnification of 3.2 through a 127-μm-diam circular pinhole. X-ray pinhole images of the pinch regions were recorded at various intensity levels over a sensitivity range of greater than three orders of magnitude. The sensitivity to x rays of the three films used increased progressively by about an order of magnitude for Kodak Fine Grain Positive (FGP), type-T, and No-Screen (NS) x-ray film. The less-sensitive films were used to examine the pinch regions while the more-sensitive ones recorded images from the less-intense flare regions.

Several films were mounted in a stacked array to record the pinch and flare structure of the exploded wires. The transmission of x rays through successive films in the array provided valuable energy discrimination since each film introduced an effective cutoff energy, below which energy the x rays were absorbed in the film. The transmission of x rays through the three types of x-ray film was determined experimentally. A 6.2-μm aluminized-Mylar foil was used to provide a light-tight cover for the film array used in the pinhole camera.

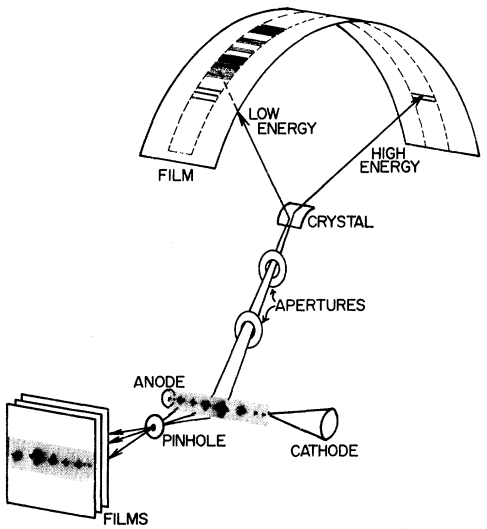

FIG. 1. Schematic of one of the crystal spectrographs and the x-ray pinhole-camera geometry used in the exploded-wire experiment.

A few x-ray images of W wires were taken with a 25-μm pinhole aperture to determine the size of the pinches. The smaller pinholes in thin metal substrates were destroyed by debris in one or two shots; therefore the larger pinhole size was used on most shots.

Two convex-curved-crystal x-ray spectrographs were used in this work to record x-ray spectra from exploded wires. A KAP (potassium acid phthlate) crystal (26.6-Å $2d$ spacing) allowed collection of data over an x-ray range of approximately 1–12 keV. The KAP crystal was elastically curved and held by adhesive tape to a metal support. The curvature of the support surface determined the radius of curvature for the KAP crystal, which was 44.2 mm. Higher-energy x-ray lines arising from inner-shell excitations were recorded in the energy range of 5 to 12 keV, with a spectrograph containing a (200) LiF (lithium-fluoride) crystal (4.02-Å $2d$ spacing). The LiF crystal was plastically curved to a radius of 3.18 mm. Both spectrographs used a geometry in which the bending axis of the crystal was parallel to the wire. The dispersed spectra were recorded on Kodak No-Screen x-ray film. The crystals and film were mounted in portable Al boxes to which were attached extension tubes for mounting the spectrograph on ports of the discharge chamber. Two circular apertures positioned at the ends of the extension tubes were used to define the length of wire from which x-ray intensity was recorded and also served to prevent radiation from the anode or chamber walls reaching the crystals. The aperture near the wire was 6.3 mm while the one nearest the crystal was 5.1 mm. The apertures used to view a portion of the exploded wire provided some limited but valuable spatial information that allowed correlation of the hot- and cool-plasma regions. A 6.2 μm Mylar film coated with 1000 Å of aluminum was placed behind the aperture inside the spectrograph box. This film prevented debris from the exploded wires reaching the crystals and also served as a light-tight window for the x-ray film.

Some of the x-ray spectral data obtained with the KAP-crystal spectrograph were recorded with a 6.2-μm-thick layer of Mylar covering one half of the film along the wavelength dispersion direction. The latitude for recording x-ray spectra on No-Screen film with this spectrograph was increased by about a factor of 10 by use of the Mylar filter. For thermal x-ray emission near

12 Å the Mylar served as an absorption foil for line radiation, while at wavelengths below ~3Å the Mylar filter substantially reduced the low-energy background radiation, resulting from total reflection from the surface of the KAP crystal, without affecting the high-energy line radiation. The same integrated spectral intensities (within the 5% level) were obtained for the thermal line emission in a W-wire shot recorded with and without the Mylar filter.

A calibration curve was constructed for converting measured spectral distances on the x-ray films recorded with the KAP-crystal spectrograph to wavelengths of x-ray energies. This curve was obtained experimentally in the 1–3.6-keV range, where most of the thermally excited spectra occurred, by use of known spectra of several of the highly ionized elements, e.g., H- and He-like lines in Al and Cl, and the Ne-like lines in Cu. In addition to spectral data, the x-ray continuum (bremsstrahlung) from the plasma produced two absorption edges on the films. These edges arose from the Al coated on the Mylar film and the K-edge absorption in the KAP crystal. They provided valuable fiducial markings at 1.599 and 3.608 keV. The empirical calibration curve was prepared from the known spectral wavelengths and the two absorption-edge energies.

Spectral data were recorded down to ~1050 eV. This cutoff was artificially imposed by the tape holding the KAP crystal; however, the effective energy cutoff from the 6.2-μm Mylar film would be about 1 keV. The precision of wavelength determination over the 1050–3608-eV energy range was ± 10 eV or at about the 1 to $\frac{1}{4}$% level. Film distances were read with a standard manual x-ray film reader. No fiducial markings appeared on the films collected with the LiF-crystal spectrograph. However all the higher-energy x-ray spectral data recorded with the LiF crystal could be interpreted by pattern recognition. Spectral data are presented in this report as densitometer tracings which were obtained with a Joyce-Loebl microdensitometer.

The experimental procedure used was to record spectral data with the two spectrographs on exploded-wire shots, read the spectral distances and convert to wavelengths, interpret the x-ray line transitions, determine the ionization states, and estimate the plasma temperatures producing x-ray spectra in both the pinches and in the cooler plasma regions that surrounded the pinches. K-, L-, and M-shell resonance-line x-ray spectra from hot plasmas generated by a focused Nd:glass laser beam, at the Naval Research Laboratory, have been collected and interpreted.[14-16] The x rays originating from ionization into the K shell in the exploded wire were readily identified by comparisons with laser data and vacuum spark data in the literature. Wires for which ionizations occurred to the L shell produced Ne-like spectra, and to the M shell produced transitions in the Ni-like isoelectronic sequences. Ionization states in these isoelectronic sequences provided extensions to the earlier work with laser-produced spectra.[15,16] In addition to extrapolation of the Ni-like isoelectronic sequence, the transitions in the tungsten exploded-wire spectra were calculated with a Dirac-Slater self-consistent-field code.[17] The plasma temperatures were estimated from the ionization states with calculations using a coronal-model code written for interpretation of the exploded-wire spectra.[18] This code calculated the distribution of ionization states for a particular element as a function of plasma temperature without incorporating dielectronic recombination. We believe the coronal-temperature estimates are accurate within a factor of 2. The coronal-model temperature estimates for the hot-thermal emission in the exploded wire are compared in Sec. IV with temperature values reported for other plasma devices producing high-ionization states.

III. RESULTS

A. Pinhole images

The x-ray pinhole images of exploded wires were found to originate from small-pinched regions and flare structure emanating from the pinches. The flares are found to be more intense on the anode side of the pinches. The Z-pinch regions and their associated flare structure arise from magnetic constrictions and $m = 0$ (sausage-type) instabilities that occur in exploded wires.[1,8] The pinches appear randomly spaced along the original wire position in the time-integrated photographs. Pinhole images of a tungsten wire are shown in Fig. 2. The pinhole photograph recorded on the less-sensitive Fine Grain Positive (FGP) film [Fig. 2(a)] shows images of the pinched regions along the original wire position. The images are seen to be pinhole limited for the 127-μm aperture. Emanating from the pinches are flares observed to have a somewhat conical shape with the pinch at the apex. This flaring structure forms an outline of the flares, seen more clearly on the more-sensitive No-Screen film in Fig. 2(c). The images on the FGP film recorded x rays primarily with photon energies > 1.05 keV, which corresponds to the effective energy cutoff of the aluminized-Mylar film placed in front of the film array. The transmission for x rays with energies below 1.05 keV is less than 10% and is the criteria used to establish the effective cutoff energy.

The images in Fig. 2(b) on the type-T film show

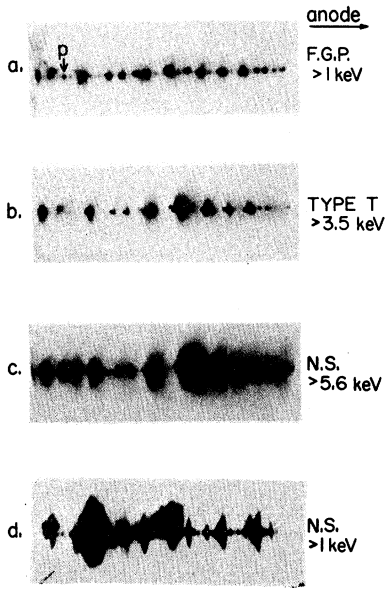

FIG. 2. Pinhole images of a W wire collected with the following film arrays after transmission through aluminized-Mylar foil: (a) Kodak Fine Grain Positive (nearest wire), (b) Kodak type T, (c) Kodak No-Screen (farthest from wire) on the same shot. The image in (d) was recorded from another W wire shot on No-Screen film (nearest wire). The various images are formed by x rays with energies above the effective cutoff values marked for each film.

more flare structure. Because of absorption in the FGP film, the pinches are less intense than on the first film even though type-T has larger AgBr grains and is approximately 8 times more sensitive than FGP for x rays (at least for x-ray energies above 4 keV). Some of the pinches seen in Fig. 2(a) are barely visible on the second film, e.g., the pinch marked *p*. Therefore the pinches emit predominately low-energy x rays with energies <3.5 keV. This cutoff value results from the measured x-ray trnasmission through the FGP which serves as a filter for the second film.

On the No-Screen (NS) film [Fig. 2(c)], the flare structure is clearly visible. For this film, which is behind the FGP and type-T films, x-ray emission above 5.6 keV is being recorded. Therefore the flares have an abundance of high-energy x-ray emission. They appear more intense on NS film because its sensitivity is about 13 times greater than type-T. No-Screen film is roughly 100 times more sensitive than FGP above 4 keV.[19] In fact, the use of a multiple NS film array indicates some flares emit a recordable emission from x rays with energies >20 keV, from tungsten wires. When a NS film is placed first in the array, as is shown in Fig. 2(d) for another W shot, we find that the flares are recordable. The size of the most intense flares recorded on the NS film placed nearest the wire range from 2–3.5 mm in diameter. Extrapolating the FGP film-sensitivity data[19] to 1 keV would indicate a sensitivity at least 10 times lower than No-Screen, whose sensitivity has been measured to 1 keV.[20] A comparison of images on NS with those on FGP when each is placed first in the film array indicates that the flares have emission in the 1–3.5-keV region but that this emission is between 10 and 100 times less intense than the <3.5-keV x-ray emission from the pinches.

We find that the spatial definition of the pinches is limited by the large aperture size of 127 μm. A 25-μm pinhole photograph revealed that the pinches for tungsten wires range in size from <25 to 75 μm. What looked like intense extended pinches in the larger-aperture images were often clusters of small pinches. The number of pinches observed in a 6.3-mm segment of wire length was typically 30 to 50.

Pinhole photographs of various wires throughout the Periodic Table are shown in Fig. 3. The emission from the Al wire is seen to be produced by large, irregularly shaped flares that extend asymmetrically from the wire axis and for distances up to 2.5 mm from the position of the pinches. The pinches can be seen clearly in the second NS film. The pinches become more collinear with increasing Z; however, the sizes of the flare structure are variable. In higher-atomic-

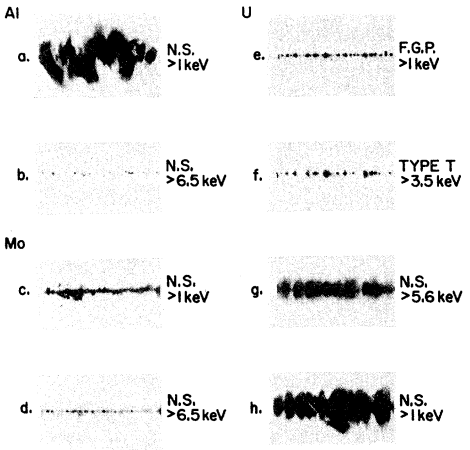

FIG. 3. Pinhole images of Al, Mo, and U wires collected with the film arrays after transmission through aluminized-Mylar foil. Al films: (a) No-Screen (nearest wire), (b) No-Screen (second film); Mo films: (c) No-Screen (nearest wire), (d) No-Screen (second film); U films: (e) Fine Grain Positive (nearest wire), (f) type T, (g) No-Screen (third film). The image in (h) was recorded from another U shot on No-Screen film (nearest wire in the array).

number wires the flares are smaller and generally emanate from the pinch symmetrically about the original wire axis. In Mo the flares are only about 400 μm in diameter, as can be seen in Fig. 3(c). There appears to be a disruptive exploded region in the first NS film for Mo [Fig. 3(c)]. The pinhole images in Mo are not as collinear as for the higher-Z wires that emit M-series spectra. The reason that the pinhole images are believed to be more collinear for high-Z wires is that radiation cooling allows the wire to explode in a less disruptive manner.[9]

The pinches are collinear for the U-wire shot, as can be seen in the FGP film, Fig. 3(e). From Fig. 3(h) the flares recorded for a U wire with NS being the first film average about 3.0 mm in diameter. It is evident that the flares in the U shot have intense, high x-ray energy emission [Fig. 3(g)].

B. X-ray spectra and plasma conditions

The x-ray spectral results from the various exploded wires will be presented element by element in order of increasing atomic number Z. The experimental results are grouped into three sections which correspond to high-temperature thermal emission from the K, L, and M atomic shells. For all the wires except Al, the x-ray spectra collected with the KAP-crystal spectrograph have lines arising from both thermal and nonthermal processes.

1. $13 \leq Z \leq 29$

The densitometer trace of an exploded Al wire recorded with the KAP-crystal spectrograph is shown in Fig. 4. The pinched regions along the exploded wire have temperatures sufficient to strip electrons from the Al atoms into the K shell, producing spectra characteristic of one- and two-electron atoms (x-ray transitions in H- and He-like states). The He-like transitions are identified as Al^{11+} (Al XII) in Fig. 4. The H-like (Lyman) transitions are identified by Greek letters. Strong satellite lines on the long-wavelength side of the resonance lines are also observed in the exploded-wire spectra similar to other Al spectra generated by hot plasmas.[14] This particular overexposed Al spectrum was chosen for analysis in order to distinguish the weak, higher-Rydberg lines. In order to make a temperature estimate, other Al spectra collected with less exposure were analyzed. The intensity of the H-like $1s - 2p$ line was about equal to the He-like $1s^2 - 1s2p$ line, which indicates a plasma temperature of higher than about 800 eV according to the coronal model. This temperature for Al corresponds to hot plasma that would produce ionization equally to these two levels. The spectrum in Fig. 4 has an intense recombination continuum seen at wavelengths shorter than the last distinct high-Rydberg Lyman ζ line in H-like ions (Al^{12+}). The thermal (Maxwellian) temperature determined from the slope of the recombination continuum intensity (after conversion from film density to exposure) was 0.65 keV. This temperature, determined from the continuum slope in the Al spectrum, is lower than coronal-model estimates obtained for both Al and higher-Z exploded-wire plasmas. The reason for this difference is not clear. An upper limit to the electron densities in the pinched regions could be estimated from the higher-Rydberg emission lines. The last distinct transition in the H-like exploded-wire spectrum is the $1s$-$7p$ line before the series is merged into the continuum. This yields, with the Inglis-Teller series-merging method, an estimated electron density of $\sim 10^{21}$ cm^{-3} for the exploded wire pinches. Comparison of the exploded-Al-wire spectrum with spectra produced by a focused laser beam indicates a higher plasma density in the exploded-wire pinches. The time-averaged electron density in the laser-produced spectra was determined to be $\sim 10^{20}$ cm^{-3} by profile analysis of high-Rydberg-series lines. Transitions from higher-Rydberg levels than are seen in Fig. 4 were recorded in laser-produced Al plasmas.

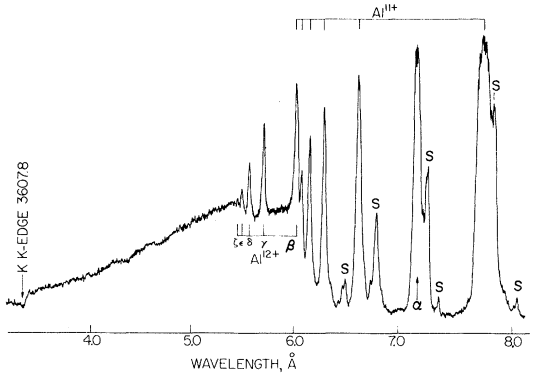

FIG. 4. Densitometer trace of an exploded-Al-wire spectrum recorded with the KAP-crystal spectrograph. The members of the H-like Lyman isoelectronic sequence are identified as α, β, γ, etc., in Al^{12+}. The long λ satellites are designed by the letter S.

A thin strip of Saran was exploded and produced a one-and two-electron Cl spectrum. This spectral pattern was similar to the Al EW spectrum and will not be discussed in detail.

Titanium spectra were collected with both the KAP and LiF-crystal spectrographs. Weak lines were measured in the KAP spectrum in the 1050- to 1170-eV range. These were transitions identified

as $1s^2 2p$-$1s^2 4d$ and $1s^2 2p$-$1s^2 5d$ in Li-like Ti XX from tables by Kelly and Palumbo.[21] Also a single line from Be-like Ti XIX was found at 1085 eV. The entire TiK spectrum was recorded with good dispersion using the LiF-crystal spectrograph. The lines found in the KAP-crystal spectrum were consistent with the pattern for the LiF-crystal spectrum. A densitometer trace of this latter spectrum and the identified ionization states are shown in Fig. 5. Radiation from high-temperature-plasma regions was found in addition to cooler-plasma emission.

The strongest, high temperature lines are the He-like lines at ~2.62 Å. The H-like lines at ~2.50 Å were a doublet with sufficient intensity to reproduce in the densitometer trace. This doublet results from spin splitting of the H-like $1s$-$2p$ lines and is shown in Fig. 5. The satellite line from Ti XXI at 2.524 Å was identified by extrapolation of the satellite-to-parent spacing from laser-produced data[22] and found to be the $1s2p\,^1P_1$-$2p^2\,^1D_2$ transition. The integrated line intensities from the Li-like and H-like states are nearly comparable to each other. The coronal temperature prediction for this ionization distribution is ~1.5 keV.

Weak lines are also found in the Ti spectrum of Fig. 5 for ionization states intermediate between the hot-plasma emission and the cooler-plasma emission (~2.74 Å). Five distinct lines corresponding to ionization states Ti XV to Ti XIX were visible on the film recorded with the LiF-crystal spectrograph. These lines were weak and difficult to obtain above the background level on the densitometer traces. The positions of these lines were carefully measured from the original film and are shown in Fig. 5 at their corresponding wavelengths.

The intense but broad line at ~2.74 Å corresponds to K-shell ionization from lower ionization states in cooler-plasma regions in addition to weak $K\alpha$ inner-shell ionization. Hartree-Fock calculations of K spectra for all sequential levels of stripping have been performed by House.[23] The calculated wavelength shift for Ti K lines between ionization states Ti II and Ti XIV is 14 mÅ, in agreement with the width of the spectral line at 2.74 Å in Ti. Most of this radiation arises from Ti XIII and Ti XIV states, from plasma regions with a temperature < 150 eV based on coronal-model calculations.

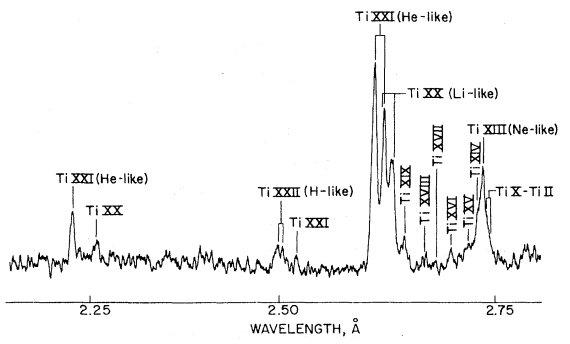

FIG. 5. Densitometer trace of an exploded-Ti-wire spectrum recorded with the LiF-crystal spectrograph.

The exploded-wire Fe spectrum recorded with the KAP-crystal spectrograph is a complex spectral pattern in the wavelength region from 7.5 to 11.6 Å. Many of the x-ray lines could be identified as belonging to Li-like Fe XXIV by comparison with solar data; however, not all of the lines have been observed from solar-flare spectra because of spectral overlap with transitions from other elements abundant in the solar atmosphere. A detailed interpretation of the exploded-wire Fe spectrum will be reported elsewhere.

The Fe K spectrum near 1.85 Å from an exploded wire was recorded with the LiF-crystal spectrograph. The physical length and breadth of the spectral lines could be correlated with the pinhole images recorded on two films simultaneously with the x-ray spectrum. The pinhole images and the Fe K spectrum are shown in Fig. 6. The upper pinhole images were recorded on Kodak FGP and No-Screen films after passing the 6.2 μm

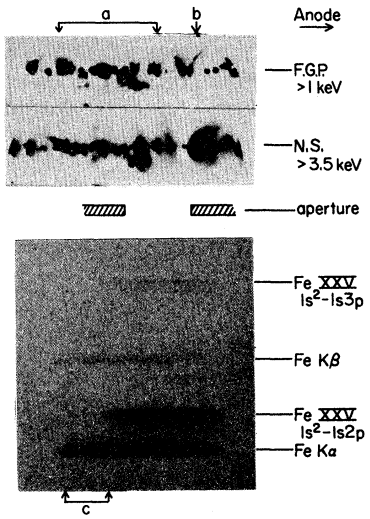

FIG. 6. X-ray pinhole images recorded on Fine Grain Positive and No-Screen film through a 127-μm-diam aperture simultaneously with the exploded-Fe-wire spectrum recorded on No-Screen film with the LiF-crystal spectrograph. The high-temperature thermal emission identified as Fe XXV arose from plasma pinches in region (a) of the pinhole images, while the portion of the Fe $K\alpha$-line region (c) arose from the intense flare at (b) seen in the pinhole image recorded on the No-Screen film.

aluminized-Mylar foil. The position of the aperture through which the x-ray spectral lines were recorded is schematically drawn in Fig. 6 between the pinhole images and the spectral pattern of the Fe $K\alpha$ spectrum recorded on No-Screen film. The intense $1s^2$-$1s2p$ transitions in Fe XXV arise from several tens of pinches located primarily in the region identified as (a) in Fig. 6. These lines are cut off on the right by one side of the aperture and on the left side the image fades because there are fewer pinches. The spectral lines from the high-temperature pinches are narrow while the inner-shell-type transitions labeled $K\alpha$ and $K\beta$ are broad. The inner-shell lines extend physically beyond the thermal lines primarily because of the intense flare located at (b). The inner-shell lines are broad both because the flare structure extends beyond about 1200 μm in diameter and because of overlapping ionization states. The spotted appearance of the Fe $K\alpha$ line at position (c) and the thermal spectral lines result from surface irregularities in the curved LiF crystal.

A densitometer trace of the Fe exploded wire is presented in Fig. 7 for the spectrum shown in Fig. 6. The high-temperature thermal spectral lines arise primarily from Fe XXIV and Fe XXV The $1s$-$2p$ transitions in H-like Fe XXVI were weakly recorded for this shot on the original NS film and appear in the densitometer trace. However, on several Fe shots the H-like lines were not recorded, possibly because fewer pinches were observed by the spectrograph. The strongest thermal lines arise from He- and Li-like states. The coronal predictions are very insensitive to the plasma temperature for Fe above 1 keV. The coronal temperature prediction for the EW spectrum of Fe is in the range from 1.2 to 2 keV.

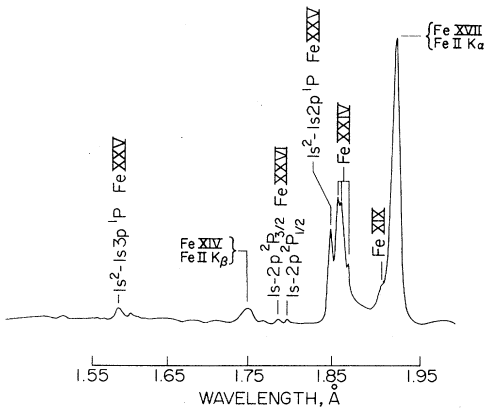

FIG. 7. Densitometer trace of the exploded-Fe-wire spectrum shown recorded on film in Fig. 6. The densitometer trace was redrawn in order to distinguish the weak lines above the fog level on the film.

Weak lines from ionization states Fe XIX to Fe XXII were found between the high-temperature Fe XXIV and Fe XXV lines and the broad line marked $K\alpha$ in Fig. 6. In the second-order spectrum, which was recorded on the same film in addition to the above-mentioned intermediate states, a line for Fe XVII was distinct. The identification of the ionization states below Fe XXIV was made on the basis of House's[23] calculations. The $K\beta$ line corresponds to the $1s$-$3p$ transition. In Fe, the highest ionization state that contains $3p$ electrons is Fe XIV. The ratio of $K\beta$ to $K\alpha$ is much less than the value normally found in inner-shell excitation because of the dominance of high ionization states such as Fe XVII. The broad line at 1.93 Å arises predominately from ionization states Fe XII to Fe XVII. The coronal temperature range for a cool plasma indicated by this distribution of ionization states is 50 to 150 eV.

In the densitometer plot (Fig. 8) of the Cu exploded-wire spectrum from the LiF-crystal spectrograph, we find distinct He- and Li-like states. The identification of the Li-like state was based on House's calculations. No evidence for H-like emission was found. A coronal model predicts nearly equal He- and Li-like states for a temperature of 1.2 keV. Emission from ionization states Cu II to Cu XXI is contained in the $K\alpha$ line at ~1.54 Å, but because the $K\beta$ is weak, there is less emission from ionization states lower than XVIII in the line at ~1.54 Å. This is consistent with the x-ray data for the exploded Cu wire collected with the KAP crystal, which consist primarily of ionization states Cu XX and Cu XXI.

2. $29 \leqslant Z \leqslant 47$

A densitometer plot of the exploded-Cu-wire spectrum collected with the KAP-crystal spectro-

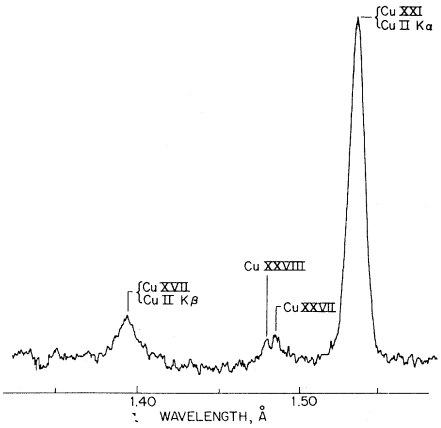

FIG. 8. Densitometer trace of an exploded-Cu-wire spectrum recorded with the LiF-crystal spectrograph.

graph is shown in Fig. 9. The spectral pattern arises from Ne-like Cu XX and F-like Cu XXI and probably lower ionization stages as evidenced from the satellite structure near the $2p^6$-$2p^5 3d$ lines. Unfortunately, the tape holding the crystal masked the $2p^6$-$2p^5 3s$ lines in Ne-like Cu at 12.558 and 12.82 Å. The $2p$-$3s$ doublet lines are the most readily recognized in the Ne-like spectral pattern. The energies shown for some of the prominent lines in Cu XX in Fig. 9 are within 5 eV of published values.[21] The coronal model predicts a plasma temperature of ~200 eV to produce Ne-like x rays in Cu.

Both Mo and Ag exploded-wire spectra were found to contain Ne-like transitions in addition to $L\alpha_1$ and $L\beta_1$ spectral lines from lower ionization states. There were also faint but visible $2p$-$3d$ lines in the Ne-like Rh spectrum produced in an exploded (Pt–13%-Rh) thermocouple wire. A densitometer trace of the Ag exploded-wire spectrum is shown in Fig. 10. The spectrum has distinct narrow Ne-like lines from Ag XXXVIII (Ag^{37+}) and an intense satellite pattern similar to that identified in the laser work with Zr.[16] There are broad lines identified as $L\alpha_1$ and $L\beta_1$ inner-shell transitions occurring in the EW spectra. The $L\beta_1$ line in Mo is shifted about 10 eV to higher energy than the value tabulated for Mo $L\beta_1$.[24] A coronal-temperature estimate for the Ag spectrum is ~1.4 keV.

3. $60 \leq Z \leq 92$

Ionization into the M shell of high-atomic-number elements produces transitions characteristic of the Ni-like isoelectronic sequence. In laser-produced rare-earth spectra, Ni-like transitions $3d^{10}$-$3d^9 4p$ and $3d^{10}$-$3d^9 4f$ and similar transitions to the $6p$ and $6f$ levels have been identified by Hartree-Slater calculations.[25] Rare-earth wires of Nd and Dy were exploded and produced spectra nearly identical to the laser-produced spectra except some higher stages of ionization were observable in the EW spectra.

Typical W spectra recorded on No-Screen film with the KAP-crystal spectrograph are shown in Fig. 11. The upper film was from a 50-μm W wire and the lower from a 25-μm-diam W wire, both exploded at the same electron potential. The x-ray spectral emission from the high-temperature pinches arises mostly from Ni-like transitions in W^{46+} that are identified in the 1.56–3.61-keV region between the Al- and K-absorption edges. The W L spectrum near 1.5 Å is recorded

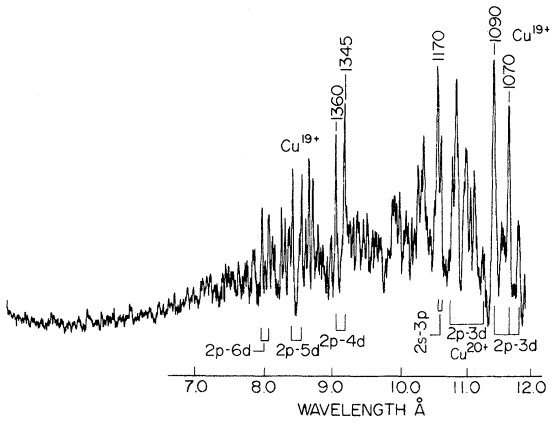

FIG. 9. Densitometer trace of an exploded-Cu-wire spectrum recorded with the KAP-crystal spectrograph. The principal transitions in Ne-like Cu^{19+} are identified below the trace. In addition the $2p$-$3d$ region in F-like Cu^{20+} is identified. The x-ray energies (in eV) are indicated above a few of the principal transitions in Cu^{19+}.

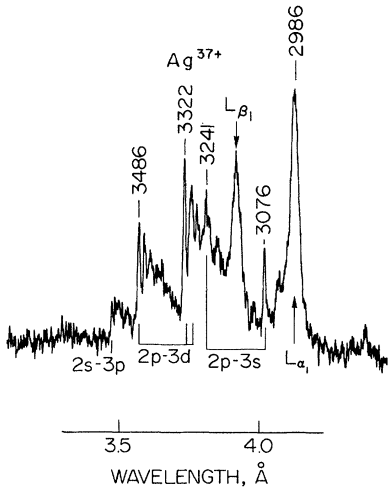

FIG. 10. Densitometer trace of an exploded-Ag-wire spectrum recorded with the KAP-crystal spectrograph. The principal Ne-like transitions in Ag^{37+} are identified together with the inner-shell $L\alpha_1$ and $L\beta_1$ lines.

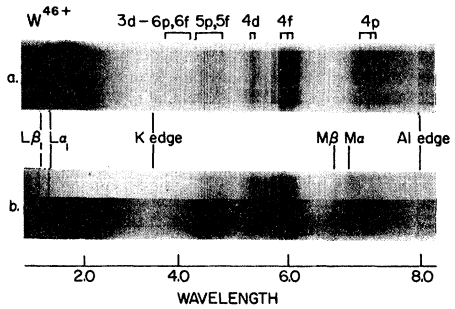

FIG. 11. X-ray spectra for exploded W wires recorded on No-Screen film with the KAP-crystal spectrograph. The W-wire diameters used in shots (a) and (b) were 25 and 50 μm. The upper half of the spectrum in (b) was recorded through a 6.2-μm-thick Mylar filter.

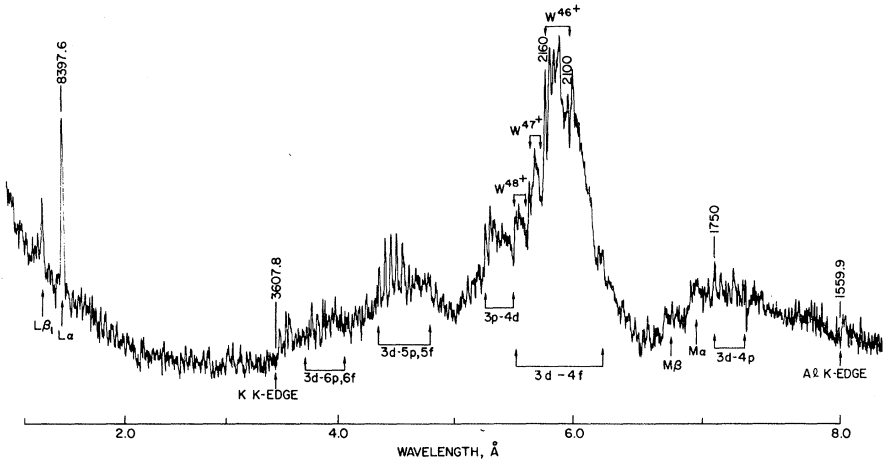

FIG. 12. Densitometer trace of an exploded-W-wire spectrum with identifications of the major Ni-like (W^{46+}) transitions in the M-series x-ray region.

with poor dispersion in the KAP-crystal spectrograph. The low-diffraction-angle background radiation beneath the W L lines in Fig. 11 results from low-energy radiation that is totally reflected from the KAP crystal. The upper half of the W spectrum in Fig. 11(b) was recorded through the 6.2-μm Mylar filter. It substantially attenuates the low-energy, totally reflected radiation in the region near the W L lines. The spectrum in Fig. 11(b) contains weak $M\alpha$ and $M\beta$ inner-shell transitions that are much broader than the high-temperature thermal lines.

A densitometer trace of the exploded-W-wire spectrum in Fig. 11(b) (behind the Mylar filter) is shown in Fig. 12 together with the identification of the spectral transitions for the Ni-like isoelectronic sequence. The W pattern was identified by Dirac-Slater calculations. The transitions in Ni-like tungsten and higher-Z exploded-wire spectra were found to be consistent with thermal M-series spectra of rare-earth elements produced by focused laser beams and lower-atomic-number elements between Cu II and Mo XV reported for vacuum spark work. The overall thermal M spectral pattern for the exploded W wire is very similar to the laser-produced spectrum for gadolinium.[15] In addition to the Ni-like W^{46+} thermal spectrum, ionization states from +44 to +49 are found in the $3d$-$4f$ region. The coronal temperature corresponding to this observed distribution of ionization states is 900 eV. Integration of the tungsten L spectral lines and integration of the total M spectral intensities between the potassium and aluminum K edges shown in Fig. 12 yielded an integrated spectral line ratio of 2% for the tungsten L to M transitions. The overall thermal M-spectral-intensity variation was at the factor of 5 level for shots in which distinct, thermal M spectra were recorded.

The L spectra produced by exploded W wires was recorded with high resolution using the LiF-crystal spectrograph. A densitometer trace of a W L spectrum is shown in Fig. 13. The resolution is sufficient to see the $L\alpha_2$ line which is separated from the $L\alpha_1$ by only 11 mÅ (62 eV). L spectra were also collected for the rare-earth elements Nd and Dy. The overall pattern both of lines and their relative intensities are nearly that of the inner-shell transitions emitted from an x-ray tube. The breadth of these lines is similar to those from the lower ionization stages in Fe and therefore indicates emission from multiple ionization states or from a broad plasma source or both.

The Pt M spectrum obtained from a thermocouple wire had distinct $3d$-$4p$ and $3d$-$4f$ lines in the Ni-like sequence superimposed on a continuum band. There was also a broad band of emission that corresponded to Co-like $3d^9$-$3d^8 4f$ transitions.

A thermal spectrum in the 3–8-Å region was obtained from an exploded, 1-mil, Au wire. The densitometer trace, Fig. 14, shows the Ni-like transitions and strong $M\alpha$ and $M\beta$ lines. These inner-shell transitions are broadened and there-

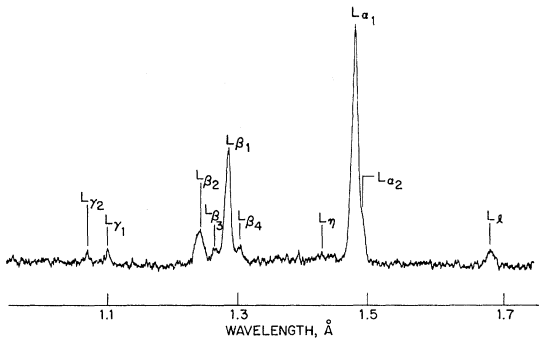

FIG. 13. Densitometer trace of an exploded-W-wire L spectrum recorded with the LiF-crystal spectrograph.

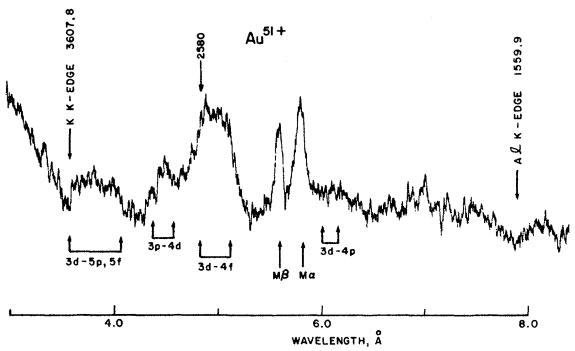

FIG. 14. Densitometer trace of an exploded-wire Au spectrum recorded with the KAP-crystal spectrograph. The Ni-like transitions in Au^{51+} and the inner-shell $M\alpha$ and $M\beta$ lines are identified.

fore arise from multiply ionized atoms. Although the thermal emission in the Au spectrum appears mainly as a continuum peak in the densitometer trace, weak but distinct, thermal lines for the $3d$-$4p$ and $3d$-$4f$ transitions in Ni-like ions were measurable in the original film. There was no distinct evidence for Co-like Au being produced. The Ni-like transitions in Au correspond to atoms 51-times ionized. The coronal-model estimate is a temperature of 1.2 keV for 51-times ionized Au.

The U spectrum consisted of broad $M\alpha$ and $M\beta$ lines, indicating multiply ionized atoms with outer-shell vacancies. The spectrum also had intense L-shell lines. There was no evidence of thermal M-shell emission, which would require temperatures in the pinches of >2 keV from coronal-model predictions.

C. Spectral wavelengths

New spectroscopic data of highly ionized high-Z x-ray spectra are available from this work. In the L-series emission, the wavelengths of the resonance transitions in the Ne-like isoelectronic sequence have been determined for Mo XXXIII and Ag XXXVIII. Wavelength data for the Ne-like transitions in exploded-wire spectra are presented in Table I. The $2p$-$3s$ and $2p$-$3d$ transitions in Mo XXXIII are found to agree, except for one $2s$-$3p$ line within 15 eV, with laser-produced spectroscopic values.[24] Since data were not available to compare with the Ag values, the Moseley diagram previously published[16] was used to extrapolate values for two transitions found in Ag XXXVIII. The agreement is within 20 eV.

The strongest M-series transitions, $3d^{10}$-$3d^9 4p$ and $3d^{10}$-$3d^9 4f$ in the Ni-like sequences, are tabulated in Table II for the high-Z exploded wires. The energies are compared with the laser-produced measurements for Dy and with values extrapolated from a Moseley diagram of Ni-like transitions.[12] The laser and exploded-wire values for transitions in Dy agree within the 15-eV experimental uncertainty in the latter data.

TABLE I. Ne-like isoelectronic sequence.

	Mo XXXIII				Ag XXXVIII			
	Exploded wire		Laser beam[a]		Exploded wire		Extrapolation	
Atomic transition	E (eV)	λ (Å)	E (eV)	λ (Å)	E (eV)	λ (Å)	E (eV)	λ (Å)
$2p^6$-$[2p^5(^2P_{3/2}), 3s]_1$	2370	5.231	2383	5.202	3076	4.031		
-$[2p^5(^2P_{1/2}), 3s]_1$	2485	4.989	2490	4.980	3241	3.825	3262	3.801
$2p^6$-$[2p^5(^2P_{3/2}), 3d(^2D_{3/2})]_1$	2555	4.852			3297	3.760		
-$[2p^5(^2P_{3/2}), 3d(^2D_{5/2})]_1$	2580	4.805	2581	4.804	3322	3.732		
-$[2p^5(^2P_{1/2}), 3d(^2D_{3/2})]_1$	2665	4.652	2678	4.630	3486	3.557	3491	3.551
$2s^2 2p^6$-$[2s2p^6 3p(^2P_{1/2})]_1$	2750	4.508	2777	4.464	3578	3.465		
-$[2s2p^6 3p(^2P_{3/2})]_1$	2775	4.468	2808	4.416				
$2p^6$-$[2p^5(^2P_{3/2}), 4s]_1$	3255	3.809						
-$[2p^5(^2P_{1/2}), 4s]_1$	3295	3.763						
$2p^6$-$[2p^5(^2P_{3/2}), 4d(^2D_{5/2})]_1$	3365	3.684						
-$[2p^5(^2P_{1/2}), 4d(^2D_{3/2})]_1$	3410	3.636						

[a] Laser-produced values, Ref. 24.

TABLE II. Transition energies for the Ni-like isoelectronic sequence from exploded-wire plasmas.

Element + ionization state	$3d^{10}$–$3d^9(^2D_{5/2})4p_{3/2}$ Expt. energy (eV)	Extrap. energy (eV)	$3d^{10}$–$3d^9(^2D_{5/2})4f_{7/2}$ Expt. energy (eV)	Extrap. energy (eV)	$3d^{10}$–$3d^9(^2D_{3/2})4f_{5/2}$ Expt. energy (eV)
Dy^{+38}	1275 ± 15	1266	1550 ± 15	1543	1585 ± 15
	1264 ± 2 [a]		1546 ± 4 [a]		1585 ± 4 [a]
W^{+46}	1750 ± 15	1764	2100 ± 15	2112	2160 ± 15
Pt^{+50}	2010	2041	2430	2426	2510
Au^{+51}	2090	2113	2510	2508	2580

[a] Laser-produced values, Ref. 16.

IV. DISCUSSION

A. Spectroscopic accuracy

The accuracy of the wavelength calibrations depended on the crystal dispersion and the number and quality of calibration points in the unknown spectra. In the laser-produced spectroscopy of highly ionized high-Z atoms, spectral lines from lower-Z targets could easily be superimposed on the unknown spectrum and accuracies of ±1–2 eV or about 0.1% were achieved.[15,16] In this exploded-wire work, one cannot accurately superimpose spectra because of the spatial variation of the wire position between shots. In this work the potassium- and aluminum-absorption edges were used as fiducial marks together with an empirical calibration curve. This achieved a precision at the ±10-eV level. An accuracy of about ±15 eV was obtained, as evidenced by the comparisons of the Mo L-series and Dy M-series line energies with those reported from laser-produced data, and also from comparisons of Ag, W, Pt, and Au transition energies with values extrapolated from Moseley diagrams. This accuracy is sufficient to identify spectra and determine ionization states but is not the desirable degree of accuracy for purely spectroscopic tabulations.

B. Spectral reproducibility

The crystal spectrograph geometries used in this work were appropriate to record the x-ray spectra from exploded wires in single shots. Improved latitude for recording x-ray spectra on No-Screen film with the KAP-crystal spectrograph was achieved using the Mylar filter. From the x-ray pinhole photography, the spectral lines from the high-temperature thermal emission resulted from 30–50 pinches in W wires, and the nonthermal W L spectra arose from a smaller number of flares. In the high-Z wire pinhole images, the number of flares, with sufficient intensity to be recorded was roughly one-half the number of distinct pinches. Within the limits imposed by the spectrograph geometries and the latitude of film exposure both thermal and nonthermal spectra were recorded in good shots. These were shots for which the electron beam suitably coupled into the wire as judged by a relatively uniform array of collinear pinches.

Possible variations in either the distribution of ionization states or the x-ray emission from the thermal pinches were examined by comparison of M spectra from various tungsten-wire shots. The approximate relative x-ray emission was measured from densitometer traces by integrating the recorded densities of the M thermal spectra from tungsten-wire shots. The W thermal spectral distributions were integrated above the background levels of the continuum at wavelengths just below the potassium edge at 3.434 Å and the aluminum edge at 7.948 Å. This integration is seen to include all the thermal M-shell emission identified by transitions in Fig. 12. The variations of thermal x-ray emission from individual pinches in a W-wire spectra were a factor of 5. On all the shots for which thermal W spectra were recorded, ionization states from +44 to +48 could be identified in the $3d$-$4f$ region. There was a surprising constancy in the distribution of ionization states and the spectral transitions for tungsten. In other wire spectra, the ionization-level variations were slight and within one state; i.e., in the Fe data, the H-like line doublet was weakly recorded in a few shots but not detectable in others. This could result either from plasma temperature differences between shots or variations in the number of pinches from which the spectral lines were recorded in individual shots.

C. Spectral intensity trends

There are systematic variations with atomic number in spectral intensities from various atomic shells. These variations are observed as

trends in the relative intensities of the resonance-line to inner-shell emission, and they are due to the increase with Z in the binding energies of each shell, in comparison to the plasma temperature. Trends in each spectral series can be noted by systematic reexamination of the spectra.

Considering first the K-shell spectra, for Al even a cool-plasma temperature of 100 eV is sufficient to ionize into the K shell. The inner-shell $K\alpha_1$ line ($1s$-$2p$ transition in singly ionized atoms) was not observed in Al but was weakly recorded in the Cl spectrum. In Ti, however, a wide range of ionization states exist (Fig. 5) and there is significant inner-shell contribution (e.g., Ti XIII) to the spectrum. But the Ti spectrum is still predominately thermal in origin. This situation is reversed in Fe (Fig. 7), where the inner-shell transitions (Fe XVII-Fe II $K\alpha$) are the strongest features. The Fe thermal radiation (Fe XXIV-Fe XXV) is still pronounced while in the Cu spectrum (Fig. 8) there is less evidence of the thermal emission.

The L-series spectra show a similar trend. The Cu spectrum (Fig. 9) contains predominately thermal (Ne-like) radiation. In both the Mo (not shown) and Ag (Fig. 10) spectra, the high-temperature thermal emissions produce Ne-like lines and L-series satellite structure from Na- and Mg-like states. The inner-shell $L\alpha$ and $L\beta$ transitions are recorded in both these spectra. To produce these inner-shell L transitions $3d$-shell electrons must be available for which plasma temperatures are much cooler than 1.4 keV. The relative intensity ratio of inner-shell to hot-thermal emission increases going from Mo to Ag. On the basis of the ionization level distributions calculated with the coronal model, the relative increase in inner-shell to thermal-line emission would result from a less-intense high-temperature thermal emission because of the increase in the binding energies of L-shell electrons in Ag compared to Mo. The W L spectrum (Fig. 13) consists entirely of inner-shell lines as the plasma temperatures are not sufficient to produce thermal emission from the W L shell.

Fewer M-series spectra were measured, but again the decrease in thermal emission with Z can be discerned. The W M spectra (Figs. 11 and 12) are mostly thermal. The weak inner-shell $M\alpha$ and $M\beta$ lines identified for W are relatively strong in Au (Fig. 14) and constitute the entire U L spectrum (not shown).

In summary, systematic trends are observed in the exploded-wire spectra. With increasing Z, the relative intensity of cool- (inner-shell) to hot- (resonance) plasma line emission increases for transitions involving the K, L, and M shells. This results from the increase in binding energies along an isoelectronic sequence with increasing atomic number.

D. Types of x-ray emission

The x-ray pinhole images and the spatial correlation of spectral emission indicate at least three types of x-ray emission emanate from exploded-wire plasmas. These various emissions were found to be (a) hot-plasma thermal emission, (b) cool-plasma thermal emission, and (c) nonthermal emission from cool flares. These plasma sources will be discussed in this and subsections IV E and IV F.

The x-ray emissions from high-ionization states in K, L, and M spectral series are recorded as narrow lines with the KAP-crystal spectrograph. The correlations with the pinhole images indicate that the high-temperature emission is produced by the pinched regions which emit x rays predominately in the less than 3.5-keV energy region. Supporting evidence that the pinches emit x rays with 1–3-keV energies was obtained from the time histories of x-ray measurements with x-ray vacuum diode detectors combined with balanced x-ray absorption filter pairs[26] in more recent Gamble II exploded-wire experiments.

Thermal x-ray emission is also found from cooler-plasma regions with temperatures between 50 to 200 eV. This is evident from the XII–XIV ionization states in Fe and the XIII–XIV ionization states in Ti that were recorded with the LiF-crystal spectrograph. The length of the line in the Fe spectrum correlated this emission with the flare structure observed on the anode side of the pinches in the x-ray pinhole images (see Fig. 6). Supporting evidence for these ionization states was found in the Ti and Fe spectra collected with a grazing-incidence grating in the 10–200-Å region for wires exploded in the Gamble II generator.[27] The Cu L-series x-ray lines obtained with the KAP crystal indicated a plasma temperature of 200 eV to produce Ne-like transitions. In the grating data, transitions in the Na- and Mg-like isoelectronic sequences of Cu were also present, which combined with the x-ray data indicates a plasma temperature range of 150–200 eV. This is somewhat higher than the 50–150-eV cool-plasma temperature indicated for spectral patterns of elements other than Cu. The widths of the Cu L-series lines in the 7–12-Å region were equivalent to those in the same wavelength region for Fe XXIV lines. The latter lines are produced by the high-temperature pinches. In spatially

resolved Cu x-ray spectral data[28] both narrow and broadened L-series Cu lines were observed. The narrow lines were produced in regions that had a closely spaced cluster of pinches while the broadened lines arose from an intense flare region. This flare had intense emission of energetic x rays (>5 keV) and had a longer time duration than the cluster of pinches.[10]

Transitions from cool plasma are also found in higher-Z spectra. The flares seen in the pinhole images are recorded from both low- and high-energy x-ray emission. The broad, inner-shell $M\alpha$ and $M\beta$ lines that are weakly detected in a few W shots probably arise from regions of low-temperature plasma. An accurate wavelength determination of the $M\alpha$- and $M\beta$-line energies could not be made in the high-Z spectra in order to determine a possible wavelength shift arising from low-ionization states in cool plasma. The width of the $L\alpha_1$ and $L\beta_1$ lines in Mo and Ag spectra were 3 times broader than adjacent $2p$-$3s$ lines in the Ne-like thermal transitions. For these wires, the flare structure was about 400 μm in diameter, by comparison with the aperture-limited pinch size in the pinhole images. Accurate wavelength values for the Mo $2p$-$3s$ lines are available from laser data.[24] The Mo $L\beta_1$ line has an energy value between the two $2p$-$3s$ lines. The centroid of the $L\beta_1$ line is shifted 10 eV towards higher energy than for tabulated values of $L\beta_1$, indicating emission from low-ionization states. From Hartree-Slater calculations,[25] this energy shift for the $L\beta_1$ transition corresponds to atoms with 12–14 outer electrons, or most of the N shell, removed. Coronal calculations indicate a plasma temperature of about 50 eV.

In addition to hot- and cold-thermal-plasma emission, x rays can also be produced by energetic electrons in the exploded-wire discharges. The intense flare emission recorded for exploded-W shots is mainly high-energy x-ray emission. When the flares are recorded on No-Screen film placed behind a Fine Grain Positive film, the x rays recorded were more energetic than 5–6 keV. The high-energy flare emission is primarily W L emission at ~8 keV. This is consistent with spatially resolved W spectra, which showed that W L lines emanate from regions between pinches where intense flares have been recorded.[28] The higher-energy x rays from W wires have time histories of longer duration than the pinches. In x-ray streak-camera data obtained through absorption filters,[29] the higher-energy radiation (>5 keV) from W wires was broader on the anode side of the wire in a few shots. This is interpreted as plasma expansion, which corresponds to what is observed as flares in the pinhole images.

E. Pinched-plasma regions

The temperatures for the individual spectra originating from pinch regions were predicted by a coronal model without dielectronic recombination and found to be consistent within the range from 0.9 to 2.0 keV for K, L, and M spectra. The coronal-temperature estimates for the elements Cu, Ag, and Au were 1.2–1.4 keV. These elements had the highest ionization levels in the K, L, and M spectra, respectively. Since thermal M emission was not observed in exploded-U-wire spectra, the coronal model predicts that the temperature in the pinches was below 2 keV. The temperature value determined from the recombination radiation found in the Al spectrum had a lower temperature of 0.65 keV. A value of 0.9 keV was determined from bremsstrahlung continuum measurements of exploded W wires[30] for x-ray emission below 8 keV. This value of 0.9 keV agrees with the coronal-model prediction for W obtained from line spectra. The electron density determined for the pinches formed in exploded-Al-wire plasmas was $\sim 1 \times 10^{21\pm1}$ cm^{-3}. The remainder of this section will compare the high-ionization states and plasma temperature and density estimates obtained from the K, L, and M spectral patterns from the high-density-plasma pinches formed in the exploded wire with conditions in highly ionized plasma produced by other devices.

High-temperature plasma regions are found to be produced in high-density pinches formed in the vacuum-spark (VS) device.[31-38] In work with the vacuum spark, Cohen *et al.*[31] and Fraenkel and Schwob[33] obtained Fe spectra with a higher distribution of ionization states (H-like and He-like ions), which indicates a somewhat higher plasma temperature, than found in the Fe K spectrum for the exploded wire. Their highly ionized Fe spectra required between 100 to 1000 sparks and originated from irreproducible plasma pinches formed near the anode surface in the vacuum spark. Schwob and Fraenkel[34] report a plasma temperature for their Fe spectrum equal to 4 keV, from the relative intensity ratio of hydrogen- and helium-like lines based on the coronal model with dielectronic recombination. For Fe ionized into the K shell, the coronal model with and without dielectronic recombination predicts about the same distribution of ionization states.[39] In highly ionized Ni and Cu spectra reported for vacuum spark work, the He-like lines were observed but not lines from H-like states.[31, 33, 38]

Lee[35] likewise has obtained an Fe spectrum from the vacuum-spark discharge device that has a higher ratio of H- to He-like lines than produced

in the exploded wire. The highly ionized spectral lines arise from pinches that are 20–50 μm in diameter with electron densities of $\sim 10^{21\pm1}$ cm^{-3}. Active detector measurements of the bremsstrahlung continuum indicated that the plasma temperatures varied between 2 and 10 keV. A plasma temperature of 8 ± 2 keV was obtained from the bremsstrahlung profile for Fe x-ray emission above 6 keV, and also above 100 keV using a nuclear emulsion. The Fe spectra reported by Fraenkel and Schwob[33] and by Lee[35] were obtained with spatial resolution to avoid the inner-shell radiation emitted by energetic-electron bombardment of the anode. The intensity ratio of lines attributed to intermediate ionization states Fe XVIII through Fe XXIII to the He-like lines (Fe XXIV) is higher in the vacuum-spark spectra than found in the exploded-Fe-wire spectrum. The ionization states Fe XVII, Fe XVIII, Fe XIX are found to be intense in the vacuum-spark spectra, while in the exploded-wire Fe K x-ray spectrum the lines from Fe XVII and Fe XIX are weak while Fe XVIII has not been detected. Assuming these lines originate from a pinch, this distribution of ionization states could indicate that the pinched-plasma regions in the EW were closer to thermal equilibrium than the pinches produced in the vacuum spark.

The exploded-Ti-wire K spectrum has a slightly lower H-like–to–He-like line ratio than the Ti spectrum produced in the vacuum spark by Lee and Elton,[32] which again indicates a somewhat lower plasma-pinch temperature in the EW. The relative line ratios of Ti XIX to Ti XXI are about equal in the two experiments while the intermediate states Ti XV to Ti XVIII are less intense in the EW, analogous to the Fe case. Ti $K\beta$ is not present in the EW spectrum, as was the case in the VS spectrum, even though the Ti spectrum was recorded with spatial resolution in the VS experiment.

The spatial and temperature structure of the pinches and cooler-plasma sources produced in the same vacuum-spark device that was used earlier at the Racah Institute of Physics was recently studied by Feldman *et al.*[40] They collected Fe spectra with spatial resolution through an array of K-edge absorption filters. The pinched regions in the VS were determined to be ~20 μm, with plasma temperatures of 2.5 keV determined by analyzing the line intensity to continuum intensity ratios.

The high-ionization states in the exploded wire result from depositing electrical energy into micron-sized pinched regions to produce hot plasma. For the temperature range and density determined in the exploded-wire pinches, the power concentration is $\sim(1-2) \times 10^{14}$ W/cm^3. Lee[36] estimated a power concentration of $\sim 10^{15}$ W/cm^3 for the hot pinches generated in the vacuum-spark device. The size and number of pinches along the entire wire can be estimated from the x-ray pinhole images. On the average, the areal power density per pinch is 10^{15} W/cm^2, calculated from the current passing the pinch areas. This value is above the focused laser-beam irradiances reported for the spectroscopy work with the Ne- and Ni-like isoelectronic sequences.[15,16,24]

In previous laser-produced work, the L-series spectra in the Ne-like isoelectric sequence was produced[16] with a focused Nd:glass laser system at the Naval Research Laboratory. With a laser irradiance of 3×10^{14} W/cm^2, the Ne-like transitions were produced in elements as high as Zr in the Periodic Table. The coronal model predicted a plasma temperature of 0.7 keV to produce Zr XXXI. This same laser irradiance level produced a highly ionized Al spectrum with a corresponding coronal temperature of 0.7 keV. Aglitskii *et al.*[24] reached Ne-like Mo with a slightly higher laser irradiance of 5×10^{14} W/cm^2 with a Nd:glass laser. With the exploded wire, the Ne-like pattern in Mo is more distinct than the laser-produced Zr XXXI pattern. The Ne-like and satellite x-ray spectral patterns in the exploded-Ag-wire spectrum are similar to those in the Zr XXXI spectrum. Therefore higher ionization states are produced in the EW for L-series spectra than have been reported with focused laser beams. The Gamble II generator should be capable of producing Ne-like transitions to $Z = 50$ (Sn) but this has not been demonstrated.

The exploded-wire results can also be compared with Tokamak data. On the basis of a coronal prediction, the plasma temperature for the exploded-Mo-wire spectrum was 1.4 keV. The principal ionization state for the Mo spectrum was the Ne-like state with evidence of Na- and Mg-like states existing as satellite lines. These lines are on the long-wavelength side of the intense $2p$-$3d$ transitions and result from transitions in ions with $3s$ or $3p$ electrons in the ground state. Ultraviolet transitions in Mo have been measured in the TFR Tokamak device[39] as impurity atoms. These spectral lines, produced in the core of the TFR Tokamak plasma, arise from Na- and Mg-like transitions involving $3s$ electrons. A coronal temperature of 1.4 keV was predicted to produce these ionization states and agreed within ±0.4 keV with the electron temperature of the hot core of the Tokamak toroidal plasma as measured by Thomson scattering.[39]

The plasma temperature estimated from the

exploded-W-wire spectrum can be compared indirectly with the results obtained from a tungsten-doped deuterium plasma produced in a dense-plasma-focus device. The x-ray emission in the 1.5–4-keV energy range measured with balanced filters over active detectors was judged to be resonant line emission from tungsten stripped to the M shell (W^{46+}).[41] For the electron density of 3×10^{19} cm^{-3}, a coronal temperature of 1.5 keV was estimated for this tungsten-doped plasma. A density greater than 1.5×10^{20} cm^{-3} would require a lower temperature of 1 keV to be consistent with a <15-nsec time to remove all the N-shell electrons in W.[41] This corresponds to the temperature and density regime for the EW pinches.

In conclusion for this section, the coronal-model prediction of plasma temperatures from highly ionized K, L, M spectra of 0.9 to 2 keV for the pinches formed in exploded wires is consistent with the coronal temperatures obtained in other hot-plasma-generating devices. The vacuum spark has produced a slightly higher distribution of ionization states in K spectra with temperature estimates which range from 2 to 10 keV. There is agreement in the coronal-model temperatures between the EW, laser-produced, and Tokamak plasmas for L-series spectra. The coronal estimate of ~1 keV to produce W^{46+} agrees with the coronal value determined in the plasma-focus device. The electron density of $1\times10^{21\pm1}$ cm^{-3} determined for the pinches formed in Al exploded-wire spectra is consistent with the 10^{21}-cm^{-3} density value determined by Lee[35] and the value of 5×10^{20} cm^{-3} determined by Cilliers *et al.*[38] for the vacuum-spark device.

F. Cool-plasma emission

The exact spatial origin of the thermal and nonthermal x-ray emissions from cool-plasma (50–200 eV) regions is somewhat unclear. The possibility that they might be produced in pinches which are not at thermal equilibrium can be ruled out because of the correlation of the $K\alpha$ and $K\beta$ lines in the Fe spectrum with the intense flare. The length of these lines did not correlate with the length of wire where many pinches occurred, giving rise to the recordable spectral lines from the high temperatures of the pinched plasmas. Furthermore, the uniformity of ionization states formed in the plasma pinches in W wires indicates a high degree of equilibrium. In the pinhole images of wires collected on the FGP films, faint conical outlines are seen flaring from both sides of the pinches. On the anode side of the pinches, this flaring of low-energy x-ray emission outlines the higher-energy flare region formed in the subsequent films. The inner-shell low-energy x-ray emission from high-Z wires might originate in the flaring structure. The spatial evidence found for the L-series lines in Cu indicates that cool plasma is formed both in the intense flares and in regions where the pinches were formed in clusters. The overall picture that emerges is that cool plasma is formed adjacent to the pinches probably as the plasma begins expanding from the pinch restriction but where the density is still sufficient to obtain recordable spectral intensities.

In experiments with spatially resolved spectra taken with an Fe anode in the vacuum spark, Feldman *et al.*[40] observed that the cool-plasma emission in Fe spectra (transitions near 1.93 Å) emanated from regions spatially adjacent to and on the anode side of the pinched regions. This is consistent with the exploded-wire data. The pinched regions in the VS, according to the temporal measurements by Lee,[35] are first formed near the anode and then propagate towards the cathode at the speed of the plasma ion velocity. Lee[42] has also observed clusters of pinches resulting from multiple micropinches in VS discharges. In the exploded wire the pinches are formed randomly along the length of wire within a few nsec after the initiation of the discharge pulse.[10]

The origin of the inner-shell transitions $L\alpha$ and $L\beta$ in Mo and Ag and the $M\alpha$ and $M\beta$ lines in high-Z elements is not clear. The widths of these lines correspond approximately with the average flare sizes; however, the broadening of these lines can also result from multiple-ionization states.

The origin of the energetic x-ray emission is clearly from intense flares on the basis of the x-ray pinhole photographs. The source of the W L spectrum was correlated to energetic electron emission by measurement of the ratio of line to bremsstrahlung background emission. Several LiF-crystal spectrograph films of the exploded-wire W L-spectra were densitometered. The W $L\alpha_1$-line densities were converted to spectral intensities and integrated, as was the bremsstrahlung continuum adjacent to the L-series lines. The experimental ratio ranged from 350 to 950 for several W shots. The W $L\alpha_1$-line spectra were calculated with a formula given by Brown.[43] The classical bremsstrahlung emission was calculated below 100 keV with a nonrelativistic formula from Kirkpatrick and Wiedmann,[44] and above 100 keV, with a relativistic formula from Jackson[45] for various energies, assuming that the bremsstrahlung was generated by monoenergetic electron beams in thin targets. From the experimental line-to-background ratios, electron energies of 30 to 300

keV produced the tungsten L spectra.

There exist two sources of energetic electrons in the exploded-wire plasmas. These sources are the energetic discharge electrons and possible runaway electrons. The hard-x-ray emission produced by energetic electrons generally begins about 20 nsec after the beginning of the low energy x-ray emission from pinches and lasts for the duration of the pulse discharge. Energetic electrons from the pulse discharge would rapidly thermalize in high-density plasmas but could travel much farther through less-dense plasma regions. Runaway electrons that produce hard x rays with energies as much as 25 times the discharge potential are found in z-pinch-producing devices like the vacuum-spark[32] and the plasma-focus device.[41,46,47] Runaway electrons are also found in toroidal plasmas such as produced in Tokamak devices.[48,49]

The hard-x-ray emission from the energetic electrons in the exploded-wire plasma is emitted preferentially on the anode side of pinches. Examination of the x-ray pinhole photographs taken with No-Screen film in the second position reveals many isolated pinches in which essentially no hard-x-ray emission is observable on the cathode side of the pinches. However, the same pinches collected on FGP film in the first position reveal low-energy x-ray emission on both sides of the sausage neck of the $m = 0$ instability along the outline of the sausage body. Examples can be seen in the pinch and flare structure marked (b) for the Fe plasmas in Fig. 6 and can be seen by comparing the structure in Figs. 2(a) and 2(b) for W wires. Nearly equal plasma densities on both sides of the pinches are indicated by the low-energy emission. It is difficult to understand why some hard-x-ray production would not be observable on the cathode side of the pinch if produced by the discharge electrons. The anisotropy of hard-x-ray emission therefore supports the possibility that runaway electrons are produced in the pinched region with sufficient abundance to produce the observed flare structure. However, because of the complex nature of the pinched-plasma regions, a quantitative prediction of the magnitude of runaway-electron production is beyond the scope of this work. Therefore it is not possible to separate the effects of the two sources of energetic electrons in exploded-wire plasmas by the use of available, time-integrated x-ray data.

V. CONCLUSIONS

A detailed spectroscopic study has been made of the x-ray emission from wires exploded by 10^{12}-W pulse discharges of relativistic-energy electrons. Two, convex-curved-crystal spectrographs recorded x-ray spectra in exploded-wire shots for atomic numbers ≥ 13. The electron beam produced micron-sized pinches (< 25 to 75 μm in diameter) along the original wire position. These small-plasma regions emitted resonance transitions for K-, L-, and M-series x rays in highly ionized atoms. The pinched-plasma regions have thermal temperatures of $\sim 1-2$ keV, based on a coronal model for the three spectral series, and have an estimated electron density of $\sim 10^{21}$ cm^{-3}. The coronal-temperature estimate of 0.9 keV for the tungsten M thermal spectrum agreed with the value determined from the slope of the low-energy (< 8 keV) bremsstrahlung continuum measured with active detectors. The estimated electron-beam power density was $\sim 10^{15}$ W/cm^2 in the micron-sized pinches. The temperature and density of the pinched plasma in the exploded wire are similar to those formed in the vacuum-spark device and are nearly the same as formed in the plasma-focus device.

The exploded-wire x-ray spectra were collectable in single shots for the spectrograph geometries used in which 30–50 pinches were observed. The shot-to-shot distribution of ionization states and the x-ray transitions observed were surprisingly constant for any one element. This was particularly the case for exploded tungsten wires. High ionization states, up to 51-times ionized in the thermal M-series spectrum in Au and up to 37-times ionized in the thermal L-series spectrum of Ag, were observed in this exploded-wire study. These ionization states are higher than have been reported with the vacuum spark or with focused laser beams. The distribution of the highest ionization states in the exploded wire is somewhat lower in the K spectra of Ti and Fe than have been reported for the vacuum spark.

Strong inner-shell-type radiation was also observed in the exploded-wire x-ray spectra. The spatial patterns in these lines indicate that the radiation originates from cooler-plasma regions formed in the flarelike structure on the anode side of the pinched regions. Spectral lines were recorded from the expanded cool plasma (up to 3 mm in diameter) along the original wire position. Inner-shell $K\alpha$- and $K\beta$-like transitions in atoms ionized a few times were formed in Ti, Fe, and Cu plasmas from cool-plasma regions adjacent to or formed between the pinches, similar to cool-plasma x-ray emission in the vacuum spark. The coronal temperature of the cooler plasma in the exploded wire was in the 50–200-eV range.

In high-atomic-number wires, evidence exists that the inner-shell transitions in L and M spectra are formed in cool-plasma regions by energetic

electrons. In the L spectra of Mo and Ag strong $L\alpha_1$ and $L\beta_1$ lines are emitted whose maximum peak energies correspond to atoms ionized a few times. In Au and U spectra, strong $M\alpha$ and $M\beta$ inner-shell transitions are found. In both L and M series the ratio of the inner-shell intensities to the thermal spectra increase with increasing atomic number and the intensities of the inner-shell transitions are consistent with cooler-plasma temperatures. An intense W L spectrum, recorded with the LiF-crystal spectrograph, was found to be similar to inner-shell electron ionization from a cold target, as in an x-ray tube. Measurement of the W $L\alpha_1$ line to the bremsstrahlung background ratio indicates that energetic electrons in the 30–300-keV range produced the tungsten L spectrum.

ACKNOWLEDGMENTS

The authors wish to express gratitude for the support of this work by S. J. Stephanakis of the Plasma Physics Division. We express appreciation to D. B. Brown for providing the tungsten line-to-background ratio calculations. We would also like to thank D. J. Johnson for helpful discussion of the time-resolved data. The critical comments of the manuscript by D. Mosher and T. N. Lee are appreciated.

*Work sponsored by the Defense Nuclear Agency and by the CTR Division of the Energy Research and Development Administration.

[1]*Exploding Wires*, edited by W. G. Chace and H. K. Moore (Plenum, New York, 1962), Vol. I; Vol. II (1962); Vol. III (1964); Vol. IV (1968).
[2]A. E. Vlastos, J. Appl. Phys. 44, 4002 (1973).
[3]R. D. Sacks and J. A. Holcombe, Appl. Spectrosc. 28, 518 (1974).
[4]A. E. Vlastos, J. Appl. Phys. 44, 106 (1973).
[5]S. K. Händel, B. Stenerhag, and I. Holmström, Nature 209, 1227 (1966).
[6]I. M. Vitkovitsky, Phys. Fluids 7, 612 (1964).
[7]I. M. Vitkovitsky, L. S. Levine, D. Mosher, and S. J. Stephanakis, Appl. Phys. Lett. 23, 9 (1973).
[8]D. Mosher, S. J. Stephanakis, I. M. Vitkovitsky, C. M. Dozier, L. S. Levine, and D. J. Nagel, Appl. Phys. Lett. 23, 429 (1973).
[9]D. Mosher, S. J. Stephanakis, K. Hain, C. M. Dozier, and F. C. Young, Ann. N.Y. Acad. Sci. 251, 632 (1975).
[10]S. J. Stephanakis, D. J. Johnson, D. Mosher, C. M. Dozier, and J. R. Boller, Bull. Am. Phys. Soc. 20, 605 (1975).
[11]C. M. Dozier, presentation at Atomic Spectroscopy Symposium, Gaithersburg, Maryland, 1975 (unpublished).
[12]P. G. Burkhalter, presentation at Atomic Spectroscopy Symposium, Gaithersburg, Maryland, 1975 (unpublished).
[13]C. M. Dozier, P. G. Burkhalter, D. J. Nagel, S. J. Stephanakis, and D. Mosher (unpublished).
[14]D. J. Nagel, P. G. Burkhalter, C. M. Dozier, J. F. Holzrichter, B. M. Klein, J. M. McMahon, J. A. Stamper, and R. R. Whitlock, Phys. Rev. Lett. 33, 743 (1974).
[15]P. G. Burkhalter, D. J. Nagel, and R. R. Whitlock, Phys. Rev. A 9, 2331 (1974).
[16]P. G. Burkhalter, D. J. Nagel, and R. D. Cowan, Phys. Rev. A 11, 782 (1975).
[17]D. Liberman, J. T. Waber, and D. T. Cromer, Phys. Rev. 137, A27 (1965).
[18]D. Mosher, Phys. Rev. A 10, 2330 (1974).
[19]R. A. Armistead, Rev. Sci. Instrum. 45, 996 (1974).
[20]C. M. Dozier, D. B. Brown, L. S. Birks, P. B. Lyons, and R. F. Benjamin, J. Appl. Phys. 47, 3732 (1976).
[21]R. L. Kelly and L. J. Palumbo, *Atomic and Ionic Emission Lines below 2000 Angstroms*, NRL Report No. 7599 (U.S. GPO, Washington, D.C., 1973).
[22]U. Feldman, G. A. Doschek, D. J. Nagel, R. D. Cowan, and R. R. Whitlock, Astrophys. J. 192, 213 (1974).
[23]L. L. House, Astrophys. J. Suppl. Ser. No. 155, 18, 21 (1969).
[24]E. V. Aglitskii, V. A. Boiko, O. N. Krokhin, S. A. Pikuz, and A. Ya. Faenov, Quantum Electron. 1, 2067 (1974).
[25]F. Herman and S. Skillman, *Atomic Structure Calculations* (Prentice-Hall, Englewood Cliffs, N. J., 1963).
[26]D. J. Johnson, S. J. Stephanakis, and J. R. Boller, Bull. Am. Phys. Soc. 20, 659 (1975).
[27]D. J. Nagel, S. J. Stephanakis, P. G. Burkhalter, and D. Mosher, Bull. Am. Phys. Soc. 19, 944 (1974).
[28]C. M. Dozier (unpublished).
[29]D. J. Johnson (private communication).
[30]C. M. Dozier (unpublished).
[31]L. Cohen, U. Feldman, M. Swartz, and J. H. Underwood, J. Opt. Soc. Am. 58, 843 (1968).
[32]T. N. Lee and R. C. Elton, Phys. Rev. A 3, 865 (1971).
[33]B. S. Fraenkel and J. L. Schwob, Phys. Lett. 40A, 83 (1972).
[34]J. L. Schwob and B. S. Fraenkel, Phys. Lett. 40A, 81 (1972).
[35]T. N. Lee, Astrophys. J. 190, 467 (1974).
[36]T. N. Lee, Ann. N.Y. Acad. Sci. 251, 112 (1975).
[37]E. Ya. Gol'ts, I. A. Zhitnik, E. Ya. Kononov, S. L. Mandel'shtam, Sov. Phys.-Dokl. 20, 49 (1975).
[38]W. A. Cilliers, R. U. Datla, and H. R. Griem, Phys. Rev. A 12, 1408 (1975).
[39]EQUIPE TFR, Nucl. Fusion 15, 1053 (1975).
[40]U. Feldman, S. Goldsmith, J. L. Schwob, and G. A. Doschek, Astrophy. J. 201, 225 (1975).
[41]D. J. Johnson, J. Appl. Phys. 45, 1147 (1974).
[42]T. N. Lee, Bull. Am. Phys. Soc. 20, 1235 (1975).
[43]D. B. Brown, in *CRC Handbook of Spectroscopy*, edited by J. W. Robinson (Chemical Rubber, Cleveland, Ohio, 1974), p. 248, Vol. I.
[44]P. Kirkpatrick and L. Wiedmann, Phys. Rev. 67, 321 (1945).
[45]J. D. Jackson, *Classical Electrodynamics*, 3rd ed. (Wiley, New York, 1962), pp. 505–534.

[46]J. H. Lee, D. S. Loebbaka, and C. E. Roos, Plasma Phys. 13, 347 (1971).
[47]W. L. Harries, J. H. Lee, and D. R. McFarland, Bull. Am. Phys. Soc. 20, 1370 (1975).
[48]H. Knoepfel and S. J. Zweben, Phys. Rev. Lett. 35, 1340 (1975).
[49]S. von Goeler *et al.*, in *Proceedings of the Third International Symposium on Toroidal Plasma Confinement, Garching, Germany 1973* (Max-Planck-Institut Fur Plasmaphysik, Garching, Germany, 1973).

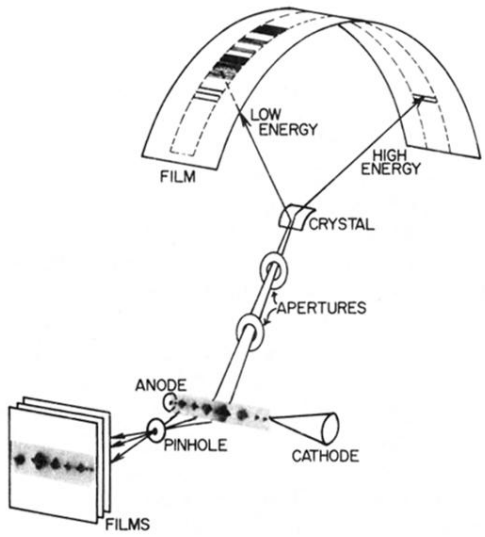

FIG. 1. Schematic of one of the crystal spectrographs and the x-ray pinhole-camera geometry used in the exploded-wire experiment.

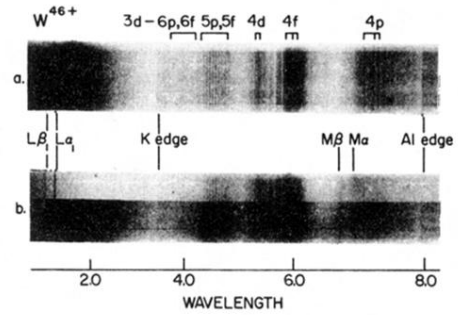

FIG. 11. X-ray spectra for exploded W wires recorded on No-Screen film with the KAP-crystal spectrograph. The W-wire diameters used in shots (a) and (b) were 25 and 50 μm. The upper half of the spectrum in (b) was recorded through a 6.2-μm-thick Mylar filter.

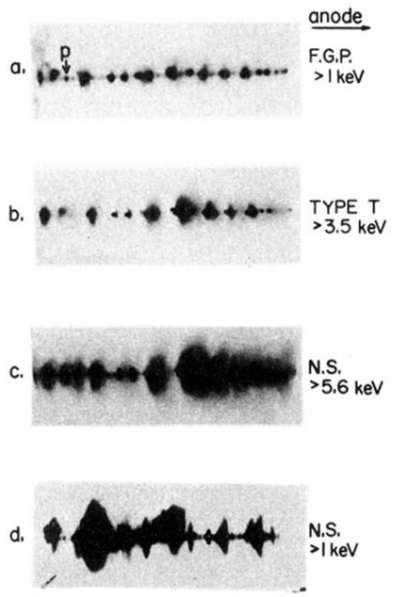

FIG. 2. Pinhole images of a W wire collected with the following film arrays after transmission through aluminized-Mylar foil: (a) Kodak Fine Grain Positive (nearest wire), (b) Kodak type T, (c) Kodak No-Screen (farthest from wire) on the same shot. The image in (d) was recorded from another W wire shot on No-Screen film (nearest wire). The various images are formed by x rays with energies above the effective cutoff values marked for each film.

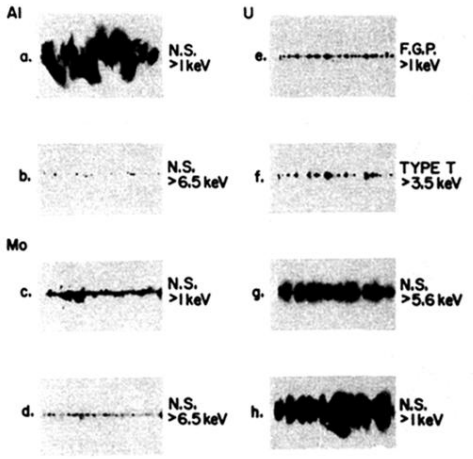

FIG. 3. Pinhole images of Al, Mo, and U wires collected with the film arrays after transmission through aluminized-Mylar foil. Al films: (a) No-Screen (nearest wire), (b) No-Screen (second film); Mo films: (c) No-Screen (nearest wire), (d) No-Screen (second film); U films: (e) Fine Grain Positive (nearest wire), (f) type T, (g) No-Screen (third film). The image in (h) was recorded from another U shot on No-Screen film (nearest wire in the array).

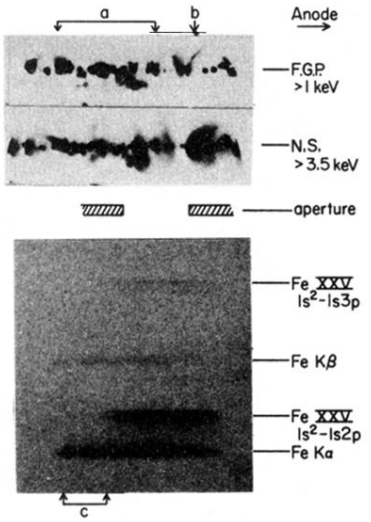

FIG. 6. X-ray pinhole images recorded on Fine Grain Positive and No-Screen film through a 127-μm-diam aperture simultaneously with the exploded-Fe-wire spectrum recorded on No-Screen film with the LiF-crystal spectrograph. The high-temperature thermal emission identified as Fe XXV arose from plasma pinches in region (a) of the pinhole images, while the portion of the Fe $K\alpha$-line region (c) arose from the intense flare at (b) seen in the pinhole image recorded on the No-Screen film.